



Cite this: *Metallomics*, 2016, 8, 920

Received 1st July 2016,  
Accepted 11th August 2016

DOI: 10.1039/c6mt00148c

[www.rsc.org/metallomics](http://www.rsc.org/metallomics)

# A systems biology approach reveals new endoplasmic reticulum-associated targets for the correction of the ATP7B mutant causing Wilson disease†

Mafalda Concilli,‡ Simona Iacobacci,‡ Giancarlo Chesi, Annamaria Carissimo and Roman Polishchuk\*

Copper (Cu) is an important trace element required for the activity of essential enzymes. However, excess Cu compromises the redox balance in cells and tissues causing serious toxicity. The process of disposal of excess Cu from organisms relies on the activity of Cu-transporting ATPase ATP7B. ATP7B is mainly expressed in liver hepatocytes where it sequesters the potentially toxic metal and mediates its excretion into the bile. Mutations in the *ATP7B* gene cause Wilson disease (WD), which is characterized by the accumulation of toxic Cu in the liver due to the scarce expression of ATP7B as well as the failure of ATP7B mutants to pump Cu and/or traffic to the Cu-excretion sites. The most frequent ATP7B mutant, H1069Q, still presents a significant Cu-transporting activity, but undergoes retention within the endoplasmic reticulum (ER) where the mutant is rapidly degraded. Expression of this ATP7B mutant has been recently reported to activate the p38 and JNK stress kinase pathways, which, in turn, trigger quality control mechanisms leading to the arrest of ATP7B-H1069Q in the ER and to the acceleration of its degradation. However, the main molecular players operating in these p38/JNK-dependent ER quality control pathways remain to be discovered. By using a combination of RNAseq, bioinformatics and RNAi approaches, we found a cluster of ER quality control genes whose expression is controlled by p38 and JNK and is required for the efficient retention of the ATP7B-H1069Q mutant in the ER. Silencing these genes reduced the accumulation of the ATP7B mutant in the ER and facilitated the mutant sorting and export to the Golgi and post-Golgi copper excretion sites. In sum, our findings reveal the ER-associated genes that could be utilized for the correction of ATP7B mutants and, hence, for the normalization of Cu homeostasis in Wilson disease.

## Significance to metallomics

Proteostasis of metal transporters plays a key role in maintaining metal homeostasis in health and disease. The current genome-wide study reveals the molecular network that regulates the ER-retention and degradation of the most frequent ATP7B mutant, which causes toxic accumulation of copper in Wilson disease. Targeting this proteostatic network with specific siRNAs corrects the ATP7B-mutant localization and, therefore, could be employed to normalize Cu homeostasis in liver cells. Our study provides new insights into understanding the interplay between ER quality control and copper transport mechanisms in Wilson disease.

radical scavenging, connective tissue biogenesis and neuropeptide production.<sup>1–4</sup> Under certain conditions, however, excess copper ions generate toxicity and compromise the redox homeostatic mechanism. The toxicity of Cu becomes particularly clear in Wilson disease, a pathological condition caused by mutation in the *ATP7B* gene.<sup>5</sup>

ATP7B encodes Cu-transporting P-type ATPase that is mainly expressed in the liver and to a lesser extent in some extra-hepatic tissues.<sup>6–8</sup> Under normal conditions, ATP7B resides in the trans-Golgi network (TGN) of hepatocytes, where it loads Cu on the newly synthesized Cu-dependent proteins, such as ceruloplasmin and hepcidin.<sup>9</sup> In response to elevated Cu, ATP7B traffics from the TGN to the endo-lysosomal organelles where ATP7B sequesters the excess metal and facilitates its excretion *via* a tightly regulated exocytic process at the biliary surface of hepatocytes.<sup>10</sup>

Wilson disease-causing mutations damage the trafficking of ATP7B to the canalicular pole of hepatocytes and/or ability of ATP7B to pump Cu across the membrane.<sup>9,11</sup> This leads to the arrest of Cu excretion into the bile and, hence, to the buildup of the metal, inducing cell death and Cu accumulation in extra-hepatic tissues. Therefore, patients affected by Wilson disease often exhibit hepatic abnormalities as well as neurological and psychiatric symptoms.<sup>5,12</sup> When left untreated, liver failure may result in death.<sup>5,12</sup>

A number of ATP7B mutations, comprising the most frequent H1069Q and R778L, still result in active ATP7B protein

## Introduction

Copper is used as a cofactor by several important enzymes that operate in a number of vital processes, such as respiration, free

Telethon Institute of Genetics and Medicine (TIGEM), Via Campi Flegrei 34, Pozzuoli, NA, 80078, Italy. E-mail: [polish@tigem.it](mailto:polish@tigem.it)

† Electronic supplementary information (ESI) available. See DOI: 10.1039/c6mt00148c

‡ These authors contributed equally to this paper and are listed in alphabetical order.

products,<sup>13–15</sup> which, however, are subjected to retention in the endoplasmic reticulum (ER).<sup>16,17</sup> Thus, regardless of the ability to transport Cu, these mutants fail to reach the Cu excretion sites and to clear excess Cu from hepatocytes.

Both mis-folding and increased aggregation do not allow ATP7B mutants to pass ER quality control checks and, thus, to be sorted into the secretory pathway.<sup>16–18</sup> Only a few components of the protein quality control machinery, which are involved in the retention and degradation of ATP7B mutants, have been identified.<sup>18–20</sup> In contrast to the similar  $\Delta 508F$  mutant of the Cystic Fibrosis Transmembrane conductance Regulator (CFTR), the regulation of the proteostatic network dealing with ATP7B mutants remains poorly understood. In this context, a recent study indicates that the expression of ER-retained ATP7B mutants triggers the activation of the p38 and JNK stress kinase pathways.<sup>21</sup> This, in turn, leads to the enhanced arrest and further degradation of the mutants in the ER.<sup>21</sup> In contrast, the suppression of p38 and JNK signalling with specific inhibitors or RNAi renders the ER quality control machinery less stringent towards aberrant ATP7B variants and allows mutants to escape towards the Golgi and post-Golgi compartments. As a result, the delivery of the ATP7B mutant to the Cu excretion sites strongly attenuates the toxic accumulation of the metal.<sup>21</sup> Therefore, targeting the ER quality control system emerges as a promising approach for the correction of the ATP7B mutant and curing of Wilson disease.

Although p38/JNK-mediated mechanisms contribute to the arrest of the ATP7B mutant in the ER, the molecular components of this mechanism remain poorly understood. The identification of downstream p38/JNK targets that hold the ATP7B mutant in the ER and direct it to degradation is of great importance. Targeting p38 and JNK for mutant correction could be associated with several risks as these kinases are involved in a broad range of cellular processes.<sup>22–24</sup> Instead, p38/JNK effectors that specifically deal with ATP7B mutants (or a restricted set of similar mis-folded proteins) would represent a pool of safer candidates for the correction strategy due to the limited impact on overall ER proteostasis.

The involvement of p38 and JNK in the regulation of the ER quality control system is well documented.<sup>22,24,25</sup> It consists of the direct phosphorylation of proteins operating in ER folding, sorting and degradation. Alternatively, the kinases could control the expression levels of key ER quality control components through transcriptional mechanisms.<sup>24,25</sup> Notably, the correction of the ATP7B mutant with p38 and JNK antagonists operates through targeting such transcriptional mechanisms.<sup>21</sup> Given that p38 and JNK control extensive signalling networks with hundreds (if not thousands) of quality control proteins,<sup>22,24,25</sup> the selection of the right components of such networks as targets for the correction of ATP7B mutants represents a serious challenge.

We used a systems biology approach to find the effectors of the p38 and JNK pathways that play a key role in ATP7B mutant retention. By analyzing the impact of p38 and JNK inhibitors on the transcriptome in ATP7B-H1069Q expressing cells, we found a cluster of ER-associated genes that were downregulated by both inhibitors. Moreover, we found that suppressing individual genes within the cluster reduced the ER retention of the ATP7B

mutant and facilitated its export into the biosynthetic pathway. This finding indicates these ER quality control components as promising targets for the correction of ATP7B mutant localization and function and, hence, for the normalization of Cu metabolism in Wilson disease.

## Materials and methods

### Antibodies, reagents, DNAs and adenoviruses

The following antibodies were used: anti-TGN46 from AbD Serotec (Oxford, UK) and secondary Alexa Fluor 568-conjugated antibodies from Invitrogen-Life Technologies (Grand Island, USA). Recombinant adenoviruses containing ATP7B-GFP or ATP7B<sup>H1069Q</sup>-GFP were previously reported.<sup>10,21</sup>

### Cell culture, treatments and adenoviral infection

HeLa cells and HepG2 cells were grown in Dulbecco's modified Eagle's medium (DMEM) with FCS 10% (decomplemented for HepG2 cells), 2 mM L-glutamine, penicillin/streptomycin. To inhibit p38 or JNK, specific inhibitors SB202190 (Sigma Aldrich, St. Louis, USA) or SP600125 (Sigma Aldrich, St. Louis, USA) were added to the cells for 24 hours at final concentrations of 10  $\mu$ M or 2  $\mu$ M, respectively. The HeLa or HepG2 cells were infected with first generation adenovirus containing ATP7B-GFP or ATP7B<sup>H1069Q</sup>-GFP, respectively, with a multiplicity of infection (MOI) of 50 and 200 virus particles per cell, respectively.

### RNA seq

Untreated as well as SB202190- or SP600125-treated HepG2 cells, expressing ATP7B<sup>H1069Q</sup>-GFP after adenoviral infection, were subjected to RNAseq. Briefly, we extracted the total RNA from the SB202190- or SP600125-treated HepG2 cells and compared them with the untreated cell line. The ribosomal RNA (rRNA) was reduced using a hybridization/bead capture procedure (Illumina TruSeq Ribo Zero). Whole-transcriptome analysis with total RNA sequencing (total RNA-Seq) was performed to detect gene subtle expression changes, alternative splice isoforms, and novel transcripts in both coding and non-coding RNA species. All the experiments were performed in triplicate with at least 50 M of paired-end reads ( $2 \times 100$  nt). The internal Next Generation Sequencing (NGS) Facility at TIGEM performed the study using an Illumina HiSeq 1000. The data obtained were further analyzed by the TIGEM Bioinformatics Core. The reads were aligned and assigned to Gencode Human transcripts and genes (release 19) by using RSEM version 1.2.19 with standard parameters.<sup>26</sup> All genes with 1 count per million in at least three samples were retained for further analysis. Differential expression analysis of read counts was performed using the Generalized Linear Model approach for multiple groups implemented in the Bioconductor package "edgeR".<sup>27</sup> The *p*-value was corrected for multiple hypothesis testing using the Benjamini-Hochberg<sup>28</sup> procedure. All genes with False Discovery Rate (FDR) below 0.01 were counted as differentially expressed.

### Gene ontology enrichment and STRING analysis

Differentially expressed genes that passed all of the above-described filtering criteria were entered into the Gene Functional Annotation Tool that is available at the Database for Annotation Visualisation and Integrated Discovery (DAVID) website (<http://david.abcc.ncifcrf.gov>) using their official gene symbols. The gene ontology (GO) options GOTERM\_BP\_ALL, GOTERM\_MF\_ALL, GOTERM\_CC\_ALL and KEGG\_PATHWAY were selected for enrichment analyses and a functional annotation chart was generated. A maximum *p* value of 0.01 was chosen to select only the significant categories. The STRING 9.1 database was utilized to analyze connections between differentially expressed ER genes and to evaluate GO enrichments within the resulting gene networks.<sup>29</sup>

### RNA interference

HeLa cells expressing ATP7B<sup>H1069Q</sup>-GFP were treated with specific siRNAs targeting: ERN1 (SASI\_Hs01\_00194923, SASI\_Hs01\_00194927), ERO1LB (SASI\_Hs01\_00126045, SASI\_Hs02\_00352900), HERPUD1 (SASI\_Hs01\_00063929, SASI\_Hs01\_00063928), SCL33A1 (SASI\_Hs01\_00198067, SASI\_Hs01\_00198068), TRAPPC6A (SASI\_Hs01\_00029309, SASI\_Hs02\_00356599), PDIA5 (Hs02\_00342340, Hs01\_00231330), HSP1A/B (SASI\_Hs01\_00051449, SASI\_Hs01\_00051450), DNAJB9 (SASI\_Hs01\_00189729, SASI\_Hs01\_00189728), CAMLG (SASI\_Hs01\_00023693, SASI\_Hs01\_00023694), EDEM3 (SASI\_Hs02\_00357963, SASI\_Hs01\_00038895) and ARL6IP1 (SASI\_Hs01\_00233782, SASI\_Hs01\_00233777). The siRNAs were purchased from Sigma-Aldrich (St. Louis, USA) and transfected using Oligofectamine (Invitrogen, Carlsbad, USA). The efficiency of silencing was checked using QRT-PCR. For this, the total RNAs from control cells and silenced HeLa cells were purified using the QIA shredder and extracted using the RNeasy Protect Mini Kit. The total RNA was converted into cDNA using the QuantiTect Reverse Transcription Kit. Q-PCR experiments were performed using the LightCycler 480 Syber Green MasterMix for cDNA amplification and the LightCycler 480 II for signal detection. The Q-PCR results were analyzed using the comparative Ct method normalized against the housekeeping gene  $\beta$ -actin. siRNA-treated cells were prepared for confocal microscopy to analyze the intracellular distribution of ATP7B<sup>H1069Q</sup>-GFP.

### Immunofluorescence and confocal microscopy

For immunofluorescence analyses, control and siRNA-treated cells expressing ATP7B-GFP-WT or ATP7B-GFP-H1069Q were fixed with 4% paraformaldehyde and permeabilised in 0.02% saponin, 0.5% BSA and 50 mM ammonium chloride prior to their incubation with the primary antibody against TGN46 AbD Serotec (Oxford, UK) and secondary anti-Sheep IgG conjugates with Alexa 568 (Invitrogen-Life Technologies, Grand Island, USA). The cells were mounted in mowiol and examined using ZEISS LSM 700 or LSM 710 confocal microscopes (Carl Zeiss Microscopy GmbH, Göttingen, Germany). All confocal images were obtained using the necessary filter sets for GFP and Alexa 568 using a Zeiss Plan-Neofluor 63 $\times$  oil immersion objective (NA 1.4), with the pinhole set to 1 airy unit. For the quantification of % of cells with ATP7B-H1069Q in the endoplasmic reticulum

(ER), the pattern of the ATP7B-H1069Q signal was analyzed using the Zen 2011 software (Carl Zeiss Microscopy GmbH, Göttingen, Germany). The diffuse network-like ATP7B-H1069Q signal expanding beyond the TGN46-positive area in each individual cell was considered as the “ER pattern”. The percentage of cells with the ER pattern of ATP7B-H1069Q was quantified in individual fields (each containing approximately 20 cells). Twenty fields were counted for each treatment to generate the mean value ( $\pm$  standard deviation). The statistical significance of difference between each RNAi treatment and control was computed using “2 tail *t*-test”. A *p*-value < 0.05 was considered statistically significant.

## Results

### p38 and JNK inhibitors cause the downregulation of ER-associated genes in cells expressing the ATP7B-H1069Q mutant

Specific inhibitors of p38 (SB SB202190) or JNK (SP SP600125) have been recently shown to facilitate the sorting of ATP7B mutants from the ER into the secretory pathway and, hence, to improve the targeting of the mutants to the Golgi and post-Golgi Cu excretion sites.<sup>21</sup> In this way both inhibitors protect the ATP7B mutant from degradation and, as a consequence, attenuate the intracellular Cu accumulation.<sup>21</sup> Considering that both inhibitors correct ATP7B mutants through transcriptional mechanisms that are under control of p38 and JNK, we investigated whether the inhibitors alter the expression of genes that could impact proteostasis, sorting and trafficking of the pathogenic ATP7B variants. To this end, hepatic HepG2 cells expressing ATP7B-H1069Q were treated with either SB SB202190 or SP SP600125 using concentrations and duration that ensured the best rescue of the ATP7B mutant.<sup>21</sup> mRNA was further extracted from the treated and control cells and prepared for RNAseq. Comparison of the transcriptomes (Fig. 1A) revealed that the p38 or JNK inhibitors altered the expression of 4153 or 3725 genes, respectively (GSE80361). Such a high number of altered transcripts prompted us to employ a further strategy to narrow down the number of candidates with high potential for the rescue of the ATP7B mutant. Firstly, we focused on searching for correctors of the ATP7B mutant on the downregulated genes because the impact of gene silencing on the mutant can be easily evaluated using a RNAi approach. Then gene ontology (GO) of the downregulated genes was analyzed for each inhibitor using 4 standard DAVID GO options (see Methods): molecular function (MF), biological process (BP), cellular component (CC) and KEGG pathways. GO enrichments were calculated for each inhibitor and ranked according to their FDR-based statistical significance (see the ESI,<sup>†</sup> Tables S1 and S2). We noted the GO enrichments in the “acute inflammatory response” and “response to oxidative stress” BP categories for genes downregulated by the p38 inhibitor, while transcripts suppressed by the JNK inhibitor were enriched in the “adaptive immune response” (BP) and “MAPK pathway” (KEGG). Notably, the JNK inhibitor-treated cells also exhibited a strong downregulation of

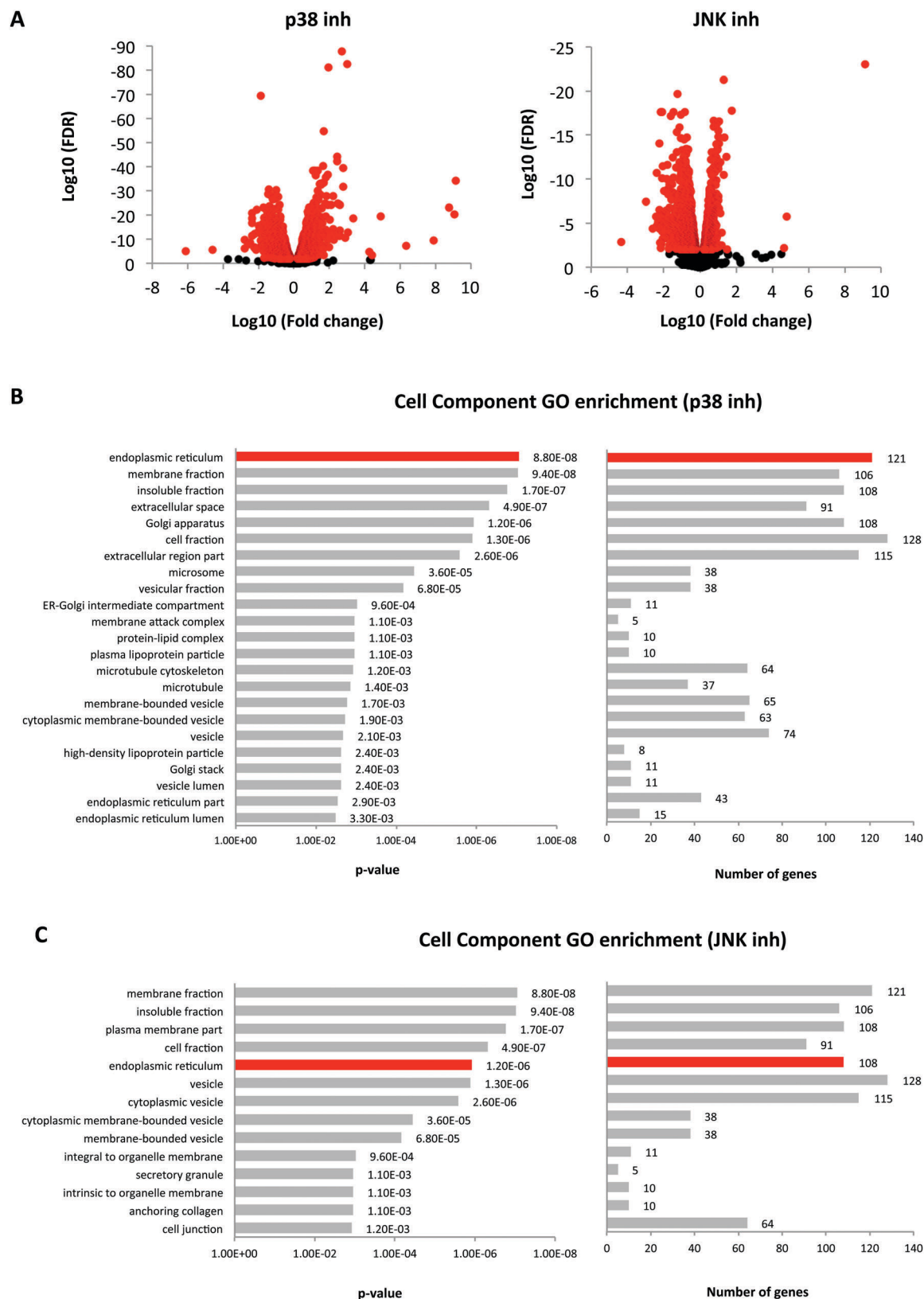


**Fig. 1** Changes in the transcriptome caused by the p38 or JNK inhibitor in ATP7B-H1069Q-expressing cells. (A) HepG2 cells expressing ATP7B-H1069Q were treated with either p38 or JNK inhibitors and subjected to RNAseq (see Methods). Graphs showing results of RNAseq analysis for each inhibitor. Differently expressed genes (FDR < 0.01) are depicted in red. (B and C) GO analysis of downregulated transcripts in p38 or JNK inhibitor-treated cells was performed using the cell component (CC) option of DAVID (see Methods). For both inhibitors tested, ER genes figured as one of the most suppressed groups according to both significance (left graphs in B and C) and number of genes (right graphs in B and C).



genes belonging to the unfolded protein response BP category. These transcriptional changes were expected because the above-listed processes and pathways frequently operate through p38 and JNK signalling.<sup>23</sup>

More importantly, CC analysis revealed significant enrichments in the ER-associated categories among the genes that were suppressed by either p38 or JNK inhibitors (Fig. 1B and C). In p38 inhibitor-treated cells, the ER-associated genes were the most downregulated CC group in terms of statistical significance and figured as one of the groups with highest number of transcripts (Fig. 1B). Similarly, in JNK-inhibitor treated cells, the ER genes represented one of the largest and most significant cohorts of suppressed transcripts (Fig. 1C). In line with these findings, our previous study indicated that inhibitors drive the correction of ATP7B mutants through ER-associated mechanisms. Therefore, we focused our analysis on these p38- or JNK-dependent groups of ER genes to find potential targets for ATP7B-H1069Q rescue.

### p38 and JNK inhibitors target a common cluster of quality control ER genes

To prioritize ER genes for further study, we took into account the previous finding that the simultaneous treatment with p38 and JNK inhibitors does not potentiate the rescue of ATP7B mutants compared to when each inhibitor is used alone.<sup>21</sup> This suggests that both inhibitors target a common pool of genes to facilitate the export of the ATP7B mutant from the ER. In this context, we investigated ER transcripts that were downregulated by both inhibitors. Fig. 2A shows that the groups of ER genes suppressed by either p38 or JNK inhibitors contain 50 common components. UniProt and PubMed annotations indicated that these 50 genes execute a wide spectrum of functions, ranging from quality control and membrane trafficking to lipid metabolism and signalling (Table 1). The degree of their downregulation by inhibitors also varied significantly (Fig. 2B). We reasoned that some of these genes could be connected into networks operating in the regulation of ER-associated processes, which, in turn, could be involved in the retention and degradation of ATP7B mutants in the ER. To test whether this was the case, the functional association of the 50 genes of interest was analyzed using the STRING database that predicts the interactions of proteins or genes on the basis of data integrated from various sources.<sup>29</sup>

The outcome of the STRING analysis was quite straightforward as two fairly big networks of genes emerged from the list of 50 ER genes (Fig. 2C). One of these networks contained genes mainly involved in lipid metabolism (green dashed line in Fig. 2C). It was difficult however to guess how the products of these genes could be involved in the retention/degradation of the ATP7B mutant in the ER. The other network was composed of ER genes associated with quality control processes (red dashed line in Fig. 2C). The core of the latter network consisted of chaperone-like molecules (HSPA1A, HSPA1B, DNAJB9 and PDIA5)<sup>30–32</sup> as well as elements of the unfolded protein response and ER-associated degradation (ERAD) machineries (ERN1, ERO1LB, HERPUD1 and EDEM3).<sup>33–35</sup> Further GO analysis revealed that the p38/JNK-dependent ER genes were enriched in the “response to unfolded proteins” and “protein processing in

ER” components. More importantly, most of these components were located within the main node of the ER quality control gene network (Fig. 2D and E) and thus represented the most suitable targets to test for the correction of ATP7B mutants.

### Silencing of p38/JNK-associated ER quality control genes results in ATP7B-H1069Q mutant rescue

The identification of the p38/JNK-sensitive cluster of ER quality control genes prompted us to test whether the suppression of these genes could facilitate the export of the ATP7B mutant from the ER. To this end, HSPA1A/B, DNAJB9, PDIA5, ERN1, ERO1LB, HERPUD1 and EDEM3 were silenced using the corresponding siRNAs in HeLa cells expressing the ATP7B-H1069Q mutant. HeLa cells were selected for RNAi experiments due to their extremely high efficiency of silencing in this cell type. In addition, we decided to inhibit other 4 ER genes, not connected with the cluster mentioned above but potentially involved in the quality control/sorting of the ATP7B mutant at the ER level according to the STRING database. These genes have been shown to regulate the shape of the ER membranes (ARL6IP1), insertion of proteins in the ER membrane (CAMLG), ER-associated protein aggregation and autophagy (SLC33A1) as well as ER-to-Golgi trafficking and sorting (TRAPP6A).<sup>36–39</sup>

Confocal microscopy revealed that control cells exhibited ATP7B-WT mainly in the perinuclear Golgi area and in a few post-Golgi vesicles (Fig. 3A1), while ATP7B-H1069Q resided within a diffuse network of ER membranes (Fig. 3A2). The silencing of ERN1, HERPUD1, PDIA5, ARL6IP1, ERO1LB, DNAJB9 and HSPA1A/B significantly reduced the retention of the ATP7B mutant in the ER facilitating its delivery to the Golgi (Fig. 3A panels 3–5, 8, 10, 11, 13), which was also confirmed by morphometric analysis (Fig. 3B). Our previous study indicates that JNK or p38 inhibitors (as well as RNAi of JNK1, p38-alpha or p38-beta) reduce the proportion of cells exhibiting the ATP7B-H1069Q mutant in the ER from ~90% to 25–40%.<sup>21</sup> Silencing individual p38/JNK-dependent genes causes a similar decrease (Fig. 3B), except DNAJB9 whose suppression has a milder impact on the ER retention of ATP7B mutant likely due to the relatively high residual expression in siRNA-treated cells (Fig. 3C). Notably, we even observed some acceleration of ATP7B-H1069Q trafficking to the post-Golgi compartments in PDIA5-depleted cells (Fig. 3A panel 5). The other siRNAs tested did not improve the export of the ATP7B mutant from the ER (Fig. 3A panels 6, 7, 9, 12). In fact, the suppression of SLC33A1 or EDEM3 rather led to the increased retention of ATP7B-H1069Q in the ER compartment (Fig. 3B). Thus, our findings indicate that almost all p38/JNK sensitive genes from the ER quality control cluster (except for EDEM3 alone) can be efficiently targeted to correct the localization of the most frequent ATP7B mutant.

## Discussion

Previous studies have indicated that the expression of aberrant forms of the Cu pump ATP7B leads to the activation of stress response pathways controlled by JNK and p38.<sup>21</sup> This activation

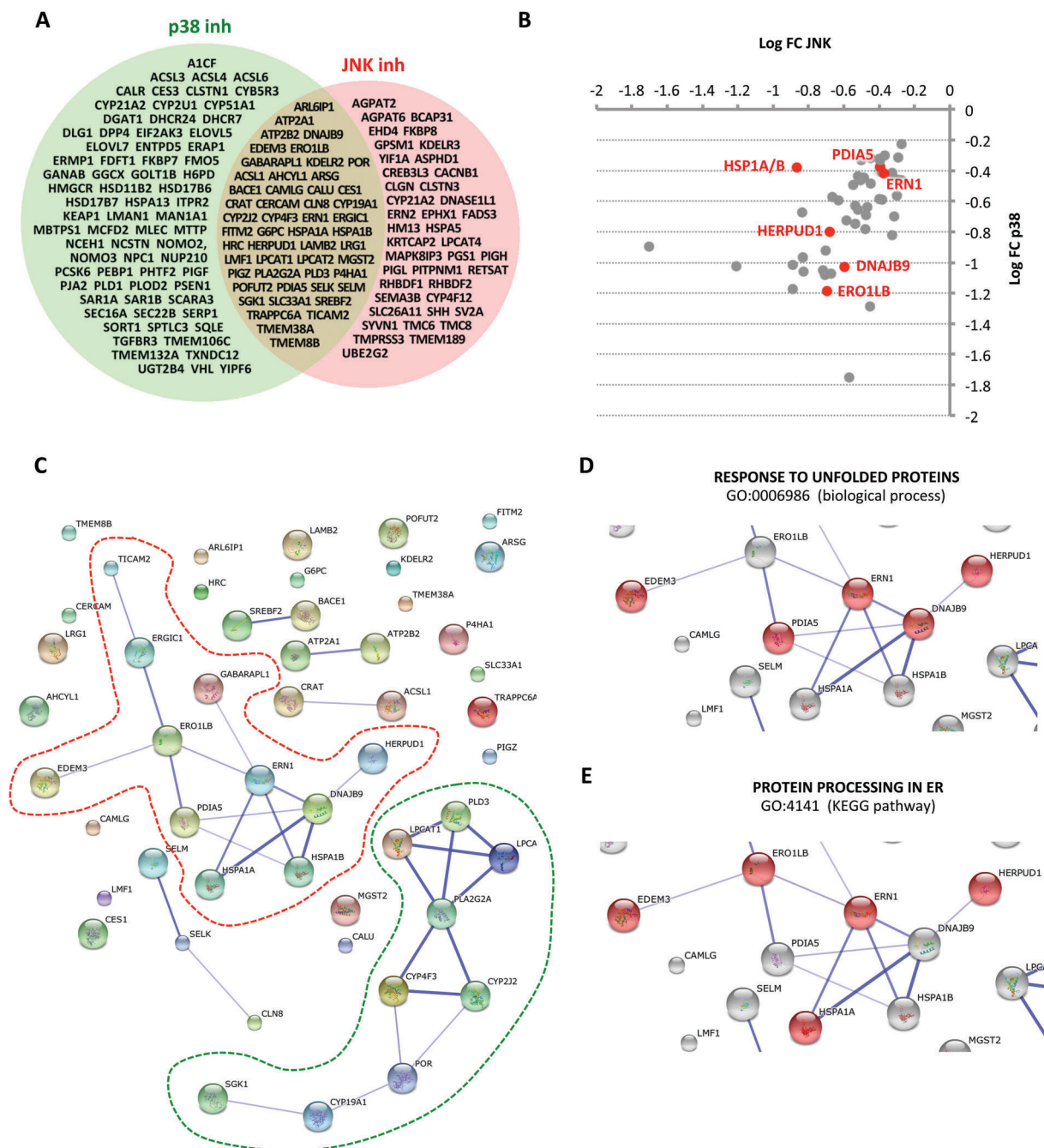


**Fig. 2** ER genes suppressed by both p38 and JNK inhibitors in ATP7B-H1069Q-expressing cells. (A) Overlap area between green and red circles shows group of 50 ER genes that are downregulated by both p38 and JNK inhibitors (see also Table 1). (B) Graph indicating the fold change (FC) in the expressed 50 genes (shown in the overlap area in panel (A)) in response to p38 or JNK inhibitors. Genes regulating ER quality control processes are shown in red. (C) p38/JNK-sensitive ER genes (shown in panels (A) and (B)) were analyzed using the STRING protein–protein interaction database (see Methods). STRING analysis revealed two large networks of interacting genes that contained components of ER quality control (surrounded by the red dashed line) or lipid metabolism (surrounded by the green dashed line). Panels (D) and (E) show the central node of the ER quality control gene network (surrounded by the red dashed line in (C)). GO analysis revealed that components of this node belong to the categories of “RESPONSE TO UNFOLDED PROTEINS” (indicated in red in panel (D)) and “PROTEIN PROCESSING IN ER” (indicated in red in panel (E)).

is likely to be triggered by both Cu-mediated oxidative damage and expression of aberrant ATP7B variants that perturb regular ER proteostasis.<sup>21,40</sup> More importantly, the suppression of either p38 or JNK leads to the rescue of ATP7B mutant localization and function that counteracts Cu accumulation in the

cells. In what way the p38 and JNK pathways mechanistically activate the degradation and retention of the ATP7B mutants and which components of the quality control machinery allow the rescue of ATP7B mutants when suppressed remain to be established.

**Table 1** List of ER-associated genes that were downregulated by both p38 and JNK inhibitors

Official gene symbol	log FC <sup>a</sup> JNK inh	log FC <sup>a</sup> p38 inh	Gene name	Function
ACSL1	−0.45	−0.48	Acyl-CoA synthetase long-chain family member 1	Lipid synthesis
AHCYL1	−0.38	−0.59	Adenosylhomocysteinase-like 1	Regulation of IP3 receptor
ARL6IP1	−0.30	−0.56	ADP-ribosylation factor-like 6 interacting protein 1	shapes ER tubules
ARSG	−0.50	−0.33	Arylsulfatase G	Lysosomal enzyme
ATP2A1	−1.70	−0.90	ATPase, Ca <sup>++</sup> transporting, cardiac muscle, fast twitch 1	ER Ca <sup>2+</sup> pump
ATP2B2	−0.45	−1.29	ATPase, Ca <sup>++</sup> transporting, plasma membrane 2	Plasma membrane Ca <sup>2+</sup> pump
BACE1	−0.53	−0.75	Beta-site APP-cleaving enzyme 1	Processing of APP
CALU	−0.27	−0.46	Calcium modulating ligand	Ca <sup>2+</sup> -mediated folding in the ER
CAMLG	−0.48	−0.45	Calcium modulating ligand	Ca <sup>2+</sup> regulation in the ER
CERCAM	−0.40	−0.32	Cerebral endothelial cell adhesion molecule	Cell adhesion
CES1	−0.47	−0.64	Calcium modulating ligand	Hydrolysis of ester- and amide-bond-containing xenobiotics and drugs
CLN8	−0.63	−0.60	Ceroid-lipofuscinosis, neuronal 8	Neuronal differentiation and in protection against cell death
CRAT	−0.30	−0.46	Carnitine acetyltransferase	Lipid metabolism
CYP19A1	−0.71	−1.08	Cytochrome P450, family 19, subfamily A, polypeptide 1	Estrogen biosynthesis
CYP2J2	−0.52	−0.44	Cytochrome P450, family 2, subfamily J, polypeptide 2	Metabolizes arachidonic acid
CYP4F3	−0.67	−1.07	Cytochrome P450, family 4, subfamily F, polypeptide 3	Lipid synthesis
DNAJB9	−0.60	−1.03	DnaJ (Hsp40) homolog, subfamily B, member 9	UPR, folding and degradation
EDEM3	−0.33	−0.82	ER degradation enhancer, mannosidase alpha-like 3	ER-associated degradation
ERGIC1	−0.29	−0.31	Cytochrome P450, family 4, subfamily F, polypeptide 3	ER-Golgi transport
ERN1	−0.38	−0.41	Cytochrome P450, family 4, subfamily F, polypeptide 3	Activates UPR
ERO1LB	−0.69	−1.18	ERO1-like beta ( <i>S. cerevisiae</i> )	ER stress, UPR
FTM2	−0.27	−0.23	Fat storage-inducing transmembrane protein 2	Fat storage
G6PC	−0.57	−1.75	Glucose-6-phosphatase, catalytic subunit	Glycosylation, energy metabolism
GABARAPL1	−0.55	−0.49	GABA(A) receptors associated protein like 3 (pseudogene); GABA(A) receptor-associated protein like 1	Autophagy
HERPUD1	−0.68	−0.80	Homocysteine-inducible, endoplasmic reticulum stress-inducible, ubiquitin-like domain member 1	ER quality control and degradation
HRC	−0.72	−1.05	Histidine rich calcium binding protein	Ca <sup>2+</sup> storage in the ER
HSPA1A	−0.87	−0.38	Heat shock 70 kDa protein 1A	Protein folding, degradation
HSPA1B	−0.87	−0.38	Heat shock 70 kDa protein 1B	Protein folding, degradation
KDELR2	−0.28	−0.47	KDEL (Lys–Asp–Glu–Leu) endoplasmic reticulum protein retention receptor 2	Retrieval of ER resident proteins from the Golgi
LAMB2	−0.33	−0.41	Laminin, beta 2 (laminin S)	Cell adhesion
LMF1	−0.89	−1.17	Lipase maturation factor 1	Lipid metabolism
LPCAT1	−0.52	−0.65	Lysophosphatidylcholine acyltransferase 1	Lipid metabolism
LPCAT2	−0.40	−0.59	Lysophosphatidylcholine acyltransferase 2	Lipid metabolism
LRG1	−0.53	−0.63	Leucine-rich alpha-2-glycoprotein 1	Leukocyte adhesion
MGST2	−0.50	−0.46	Microsomal glutathione S-transferase 2	Production of leukotrienes
P4HA1	−0.37	−0.42	Prolyl 4-hydroxylase, alpha polypeptide 1	Collagen synthesis
PDIA5	−0.40	−0.38	Protein disulfide isomerase family A, member 5	Protein folding, UPR regulation
PIGZ	−0.83	−0.67	Phosphatidylinositol glycan anchor biosynthesis, class Z	GPI-biosynthesis
PLA2G2A	−0.89	−1.02	Phospholipase A2, group IIA	Lipid metabolism
PLD3	−0.45	−0.32	Phospholipase D family, member 3	Lipid metabolism
POFUT2	−0.58	−0.73	Protein O-fucosyltransferase 2	Glycosylation
POR	−0.47	−0.69	P450 (cytochrome) oxidoreductase	Electron transfer from NADP to cytochrome P450
SELK	−0.37	−0.33	Selenoprotein K; similar to HSPC297	Regulation of ER homeostasis
SELM	−0.83	−0.97	Selenoprotein M	Selenocystein biosynthesis
SGK1	−0.48	−0.78	Serum/glucocorticoid regulated kinase 1	Regulates cellular stress response
SLC33A1	−0.37	−0.30	Solute carrier family 33, member 1	Acetyl-CoA transporter
SREBF2	−0.32	−0.70	Sterol regulatory element binding transcription factor 2	Transcription factor
TICAM2	−1.21	−1.02	Toll-like receptor adaptor molecule 2	Toll receptor signaling
TMEM38A	−0.66	−0.57	Transmembrane protein 38A	Cation channel
TMEM8B	−0.70	−0.92	Transmembrane protein 8B	Regulation of the EGFR pathway
TRAPPC6A	−0.83	−1.06	Trafficking protein particle complex 6A	ER-Golgi transport sorting

<sup>a</sup> FC stands for fold change.

In this study, using RNAseq and bioinformatics analyses, we found that p38 and JNK inhibitors downregulate a common cluster of genes that encode ER quality control components, while the suppression of these genes leads to mutant rescue. Almost all these genes have a well-documented role in the regulation of proteostasis. HSP1A/B (known also as HSP70)

operates as one of the main chaperones in ER quality control mechanisms. It arrests unfolded membrane proteins, like the ΔF508-CFTR mutant, in the ER and directs them to the ERAD.<sup>30</sup> DNAJB9 (ERdj4) belongs to the family of small chaperones that regulate HSP1A/B activity.<sup>32</sup> Recent studies have shown that the transcription of *DNAJB9* increases in response to ER stress,



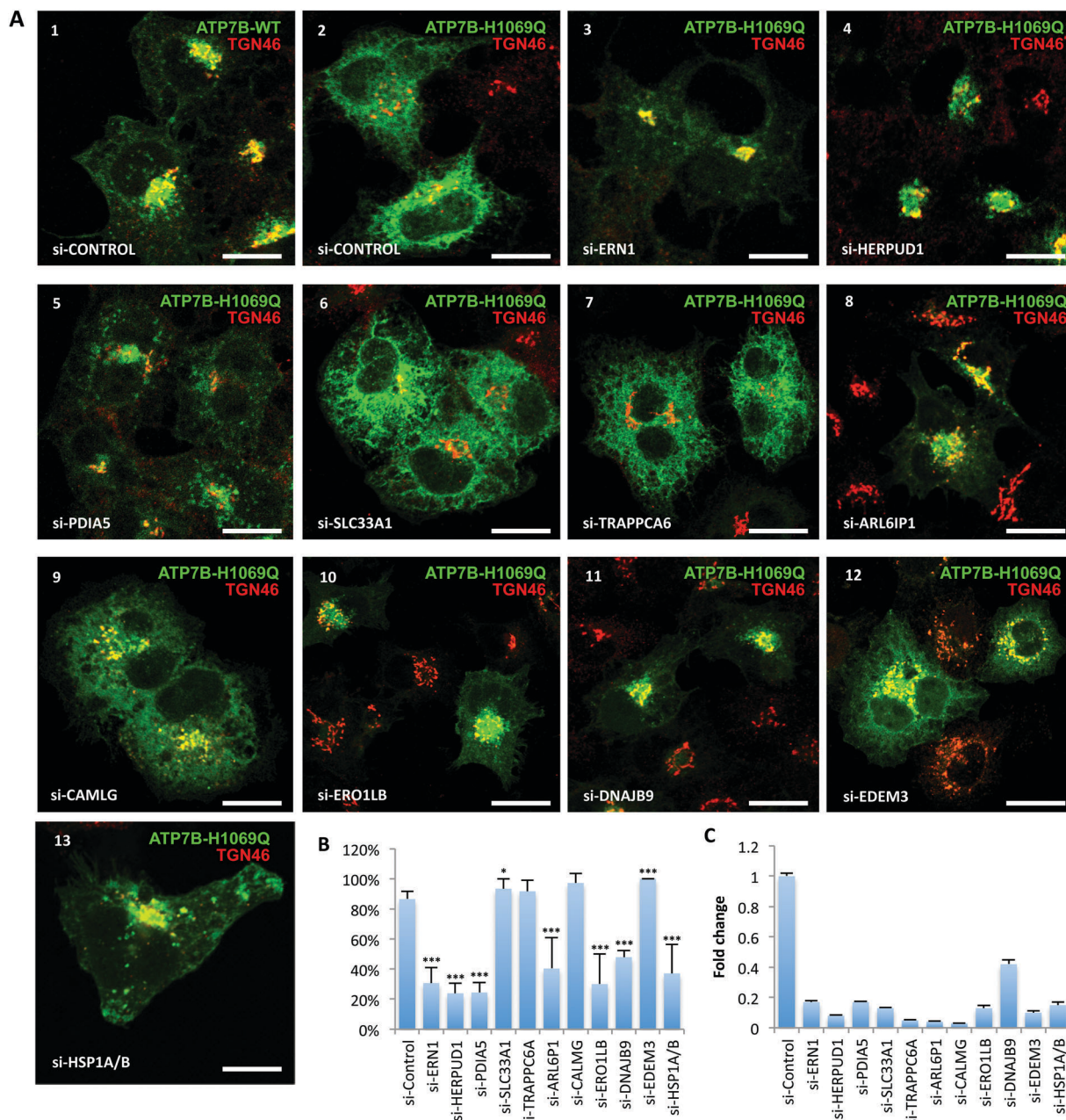


**Fig. 3** Silencing of p38/JNK-sensitive ER genes reduces the retention of ATP7B-H1069Q in the ER. (A) ATP7B-WT (panel 1) or ATP7B-H1069Q (panels 2–13) were expressed in HeLa cells using infection with corresponding adenoviruses (see Methods). Prior to infection, control or specific siRNAs were added to the cells as indicated in each panel. The cells were fixed, stained with the TGN marker, TGN46, and prepared for confocal microscopy. ATP7B-WT exhibited an overlap with TGN46 in the perinuclear area (1), while ATP7B-H1069Q was detected in a diffuse network of ER membranes (2). siRNAs targeting ERN1 (3), HERPUD1 (4), PDIA5 (5), ARL6IP1 (8), ERO1LB (10), DNAJB9 (11) or HSPA1A/B (13) reduced ATP7B-H1069Q in the ER and facilitated its delivery to the perinuclear Golgi compartment. (B) Morphometric analysis confirmed that the silencing of ERN1, HERPUD1, PDIA5, ARL6IP1, ERO1LB, DNAJB9 or HSPA1A/B decreased the percentage of cells (average  $\pm$  SD,  $n = 20$  view fields) showing ATP7B-H1069Q in the ER. (C) Cells were incubated with siRNA, which targets specific genes (indicated in the graph). The efficiency of silencing for each gene was evaluated by quantitative RT-PCR and expressed as fold-change (average  $\pm$  SD;  $n = 3$  experiments) after normalization to mRNA levels of the same gene in control cells (treated with scramble siRNA). \*  $p$ -value  $< 0.05$ , \*\*\* $p$ -value  $< 0.001$ . Scale bar: 4.7  $\mu$ m (A1–A13).

while the protein product of the gene is implicated in the ERAD by interacting with Derlin-1.<sup>41</sup> The transmembrane ER protein HERPUD1 is also controlled by UPR and interacts through its ubiquitin-like domain with the 26S proteasome. In this way HERPUD1 connects the protein degradation

machinery to the ER membrane to secure the efficiency of the ERAD process.<sup>34</sup> Finally, another UPR-sensitive gene *ERO1LB* encodes the protein that drives the oxidative protein folding.<sup>33</sup> Therefore, all the above quality control molecules are likely to be involved in the retention/degradation of the



ATP7B mutant within the ER, as revealed by the silencing experiments (Fig. 3).

However, two p38/JNK-sensitive genes that drive ATP7B-H1069Q arrest in the ER deserve particular attention. One of them, ERN1 (known also as Ire1), operates as the master-regulator of one of the main UPR pathways driving the expression of ER quality control genes.<sup>35</sup> The remaining two UPR branches are controlled by either ATF6 $\alpha$  or PERK. More importantly, another key target of p38/JNK inhibitors, PDIA5, regulates the activity within the ATF6-mediated UPR route.<sup>35</sup> PDIA5 contributes, in particular, to the disulfide bond rearrangement in ATF6 $\alpha$  under stress conditions, thereby leading to the ATF6 $\alpha$  export from the ER. The PDIA5-mediated ER export of ATF6 $\alpha$  and its further cleavage in the Golgi is required for the activation of ATF6 $\alpha$  target genes.<sup>31</sup> Therefore, it turns out that p38 and JNK inhibitors may suppress (or significantly inhibit) two of the three existing UPR pathways in hepatic cells through the downregulation of ERN1 and PDIA5. As a result, the cells cannot efficiently sense the presence of the misfolded ATP7B mutant in the ER and orchestrate its retention/degradation. This gives ATP7B-H1069Q a chance to escape the ER quality control machinery and be sorted into the secretory pathway towards the post-Golgi compartments, where the mutant has been shown to facilitate the excretion of excess Cu.<sup>21</sup> Indeed, HERPUD1, ERO1LB and DNAJ9 could constitute a core of this quality control machinery as their expression is regulated by either ATF6 $\alpha$  or Ire1,<sup>42–44</sup> while their activities are required for the ATP7B mutant capture in the ER compartment (see scheme in Fig. 4).

In addition to ER quality control genes, we found ARL6IP1 as a target for the correction of the ATP7B mutant. ARL6IP1 apparently regulates the curvature of ER membranes.<sup>38</sup> The membrane curvature could play an important role in the sorting processes as differently shaped membranes better accommodate different subsets of membrane proteins (see Polishchuk *et al.*, 2009<sup>45</sup> and reference therein). Thus, it is tempting to speculate that ARL6IP1 does not allow the ATP7B mutant to be adapted into membranes that drive the export from the ER to the distal compartments of the biosynthetic pathway, while the depletion of ARL6IP1 circumvents this sorting block. However, the mechanism through which p38 and JNK regulate ARL6IP1 expression remains to be established.

In sum, our study revealed a network of ER-associated genes that could be targeted for the rescue of the most frequent ATP7B mutant. It would be important to explore the therapeutic potential of these targets for the normalization of Cu homeostasis in Wilson disease. To this end, several issues have to be addressed in the future. The first issue is whether specific and safe drugs could be developed to regulate the expression of these genes or to inhibit the function of their products. Probably using such drugs at the right concentration and duration could still allow ATP7B-H1069Q rescue without serious side effects that could emerge in patients due to the suppression of important quality control players. Effective small molecule inhibitors of HSP1A/B have been recently reported.<sup>46</sup> However, it remains to be understood whether these inhibitors correct the ATP7B mutant and induce any serious toxicity. The second issue concerns the potential of ER gene targets for the recovery of other ER-retained

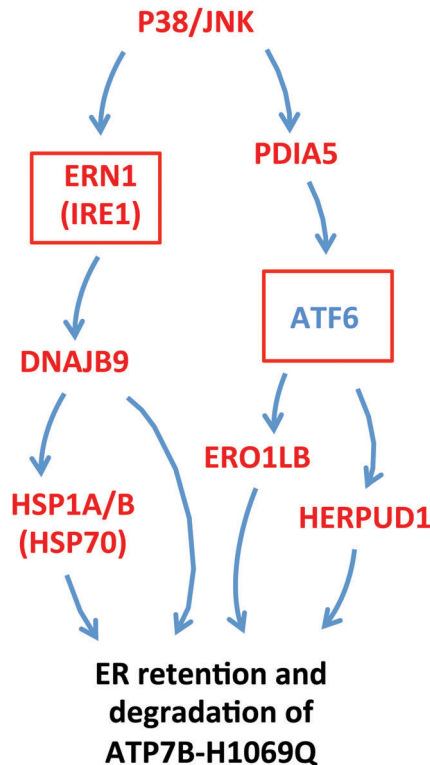


**Fig. 4** p38/JNK-dependent molecular network regulating ER retention and degradation of ATP7B-H1069Q. The scheme shows how p38 and JNK regulate a cluster of quality control genes involved in the ER retention of the ATP7B mutant. Our data indicate that both kinases may control the activity of 2 master regulators of unfolded protein response, ERN1 and ATF6 (outlined by boxes). ERN1 (Ire1) expression is upregulated by both p38 and JNK, while the activity of ATF6 could be controlled by these kinases through PDIA5. ERN1 and ATF6 activate other ER quality control components that according to our findings are required for the effective arrest of the ATP7B mutant within the ER compartment (see Discussion).

ATP7B mutants with residual activity. This would allow us to extend the “mutant correction-based” therapeutic approach to a broader range of WD patients. Indeed, small molecule correctors are usually not limited to a single ATP7B mutant.<sup>15,21</sup> In fact, we demonstrated that p38 and JNK inhibitors overcome the ER retention of several ATP7B mutants.<sup>21</sup> Thus, suppressing ER quality control genes with specific drugs could have a similar beneficial impact on different ATP7B mutants. This should also allow us to understand common and mutant-specific mechanisms that hamper ATP7B proteostasis and, hence, regulate Cu metabolism during the pathogenesis of Wilson disease.

## Acknowledgements

We would like to acknowledge the support to RP from Telethon Italy (Grant #TGM11CB4) and AIRC Italy (Grant #IG17118).

## References

- 1 J. Camakaris, I. Voskoboinik and J. F. Mercer, Molecular mechanisms of copper homeostasis, *Biochem. Biophys. Res. Commun.*, 1999, **261**, 225–232.

- 2 S. Lutsenko, Human copper homeostasis: a network of interconnected pathways, *Curr. Opin. Chem. Biol.*, 2010, **14**, 211–217.
- 3 Y. Wang, V. Hodgkinson, S. Zhu, G. A. Weisman and M. J. Petris, Advances in the understanding of mammalian copper transporters, *Adv. Nutr.*, 2011, **2**, 129–137.
- 4 T. Nevitt, H. Ohrvik and D. J. Thiele, Charting the travels of copper in eukaryotes from yeast to mammals, *Biochim. Biophys. Acta*, 2012, **1823**, 1580–1593.
- 5 J. D. Gitlin, Wilson disease, *Gastroenterology*, 2003, **125**, 1868–1877.
- 6 Y. M. Kuo, J. Gitschier and S. Packman, Developmental expression of the mouse mottled and toxic milk genes suggests distinct functions for the Menkes and Wilson disease copper transporters, *Hum. Mol. Genet.*, 1997, **6**, 1043–1049.
- 7 N. Barnes, R. Tsivkovskii, N. Tsivkovskaia and S. Lutsenko, The copper-transporting ATPases, menkes and wilson disease proteins, have distinct roles in adult and developing cerebellum, *J. Biol. Chem.*, 2005, **280**, 9640–9645.
- 8 K. H. Weiss, J. Wurz, D. Gotthardt, U. Merle, W. Stremmel and J. Fullekrug, Localization of the Wilson disease protein in murine intestine, *J. Anat.*, 2008, **213**, 232–240.
- 9 S. Lutsenko, N. L. Barnes, M. Y. Bartee and O. Y. Dmitriev, Function and regulation of human copper-transporting ATPases, *Physiol. Rev.*, 2007, **87**, 1011–1046.
- 10 E. V. Polishchuk, M. Concilli, S. Iacobacci, G. Chesi, N. Pastore, P. Piccolo, S. Paladino, D. Baldantoni, I. S. C. van, J. Chan, C. J. Chang, A. Amoresano, F. Pane, P. Pucci, A. Tarallo, G. Parenti, N. Brunetti-Pierri, C. Settembre, A. Ballabio and R. S. Polishchuk, Wilson Disease Protein ATP7B Utilizes Lysosomal Exocytosis to Maintain Copper Homeostasis, *Dev. Cell*, 2014, **29**, 686–700.
- 11 S. La Fontaine and J. F. Mercer, Trafficking of the copper-ATPases, ATP7A and ATP7B: role in copper homeostasis, *Arch. Biochem. Biophys.*, 2007, **463**, 149–167.
- 12 P. Ferenci, Review article: diagnosis and current therapy of Wilson's disease, *Aliment. Pharmacol. Ther.*, 2004, **19**, 157–165.
- 13 J. R. Forbes and D. W. Cox, Functional characterization of missense mutations in ATP7B: Wilson disease mutation or normal variant?, *Am. J. Hum. Genet.*, 1998, **63**, 1663–1674.
- 14 M. Iida, K. Terada, Y. Sambongi, T. Wakabayashi, N. Miura, K. Koyama, M. Futai and T. Sugiyama, Analysis of functional domains of Wilson disease protein (ATP7B) in *Saccharomyces cerevisiae*, *FEBS Lett.*, 1998, **428**, 281–285.
- 15 P. V. van den Berghe, J. M. Stapelbroek, E. Krieger, P. de Bie, S. F. van de Graaf, R. E. de Groot, E. van Beurden, E. Spijker, R. H. Houwen, R. Berger and L. W. Klomp, Reduced expression of ATP7B affected by Wilson disease-causing mutations is rescued by pharmacological folding chaperones 4-phenylbutyrate and curcumin, *Hepatology*, 2009, **50**, 1783–1795.
- 16 A. S. Payne, E. J. Kelly and J. D. Gitlin, Functional expression of the Wilson disease protein reveals mislocalization and impaired copper-dependent trafficking of the common H1069Q mutation, *Proc. Natl. Acad. Sci. U. S. A.*, 1998, **95**, 10854–10859.
- 17 D. Huster, A. Kuhne, A. Bhattacharjee, L. Raines, V. Jantsch, J. Noe, W. Schirrmeister, I. Sommerer, O. Sabri, F. Berr, J. Mossner, B. Stieger, K. Caca and S. Lutsenko, Diverse functional properties of Wilson disease ATP7B variants, *Gastroenterology*, 2012, **142**, 947–956e945.
- 18 M. D'Agostino, V. Lemma, G. Chesi, M. Stornaiuolo, M. Cannata Serio, C. D'Ambrosio, A. Scaloni, R. Polishchuk and S. Bonatti, The cytosolic chaperone alpha-crystallin B rescues folding and compartmentalization of misfolded multispan transmembrane proteins, *J. Cell Sci.*, 2013, **126**, 4160–4172.
- 19 S. Materia, M. A. Cater, L. W. Klomp, J. F. Mercer and S. La Fontaine, Clusterin (apolipoprotein J), a molecular chaperone that facilitates degradation of the copper-ATPases ATP7A and ATP7B, *J. Biol. Chem.*, 2011, **286**, 10073–10083.
- 20 P. de Bie, B. van de Sluis, E. Burstein, P. V. van de Berghe, P. Muller, R. Berger, J. D. Gitlin, C. Wijmenga and L. W. Klomp, Distinct Wilson's disease mutations in ATP7B are associated with enhanced binding to COMMD1 and reduced stability of ATP7B, *Gastroenterology*, 2007, **133**, 1316–1326.
- 21 G. Chesi, R. N. Hegde, S. Iacobacci, M. Concilli, S. Parashuraman, B. P. Festa, E. V. Polishchuk, G. Di Tullio, A. Carissimo, S. Montefusco, D. Canetti, M. Monti, A. Amoresano, P. Pucci, B. van de Sluis, S. Lutsenko, A. Luini and R. S. Polishchuk, Identification of p38 MAPK and JNK as new targets for correction of Wilson disease-causing ATP7B mutants, *Hepatology*, 2016, **63**, 1842–1859.
- 22 Y. Sekine, K. Takeda and H. Ichijo, The ASK1-MAP kinase signaling in ER stress and neurodegenerative diseases, *Curr. Mol. Med.*, 2006, **6**, 87–97.
- 23 M. Raman, W. Chen and M. H. Cobb, Differential regulation and properties of MAPKs, *Oncogene*, 2007, **26**, 3100–3112.
- 24 N. J. Darling and S. J. Cook, The role of MAPK signalling pathways in the response to endoplasmic reticulum stress, *Biochim. Biophys. Acta*, 2014, **1843**, 2150–2163.
- 25 R. Sano and J. C. Reed, ER stress-induced cell death mechanisms, *Biochim. Biophys. Acta*, 2013, **1833**, 3460–3470.
- 26 B. Li and C. N. Dewey, RSEM: accurate transcript quantification from RNA-Seq data with or without a reference genome, *BMC Bioinf.*, 2011, **12**, 323.
- 27 M. D. Robinson, D. J. McCarthy and G. K. Smyth, edgeR: a Bioconductor package for differential expression analysis of digital gene expression data, *Bioinformatics*, 2010, **26**, 139–140.
- 28 A. Reiner, D. Yekutieli and Y. Benjamini, Identifying differentially expressed genes using false discovery rate controlling procedures, *Bioinformatics*, 2003, **19**, 368–375.
- 29 A. Franceschini, D. Szklarczyk, S. Frankild, M. Kuhn, M. Simonovic, A. Roth, J. Lin, P. Minguez, P. Bork, C. von Mering and L. J. Jensen, STRING v9.1: protein–protein interaction networks, with increased coverage and integration, *Nucleic Acids Res.*, 2013, **41**, D808–815.
- 30 J. A. Coppinger, D. M. Hutt, A. Razvi, A. V. Koulov, S. Pankow, J. R. Yates, 3rd and W. E. Balch, A chaperone

- trap contributes to the onset of cystic fibrosis, *PLoS One*, 2012, **7**, e37682.
- 31 A. Higa, S. Taouji, S. Lhomond, D. Jensen, M. E. Fernandez-Zapico, J. C. Simpson, J. M. Pasquet, R. Schekman and E. Chevet, Endoplasmic reticulum stress-activated transcription factor ATF6alpha requires the disulfide isomerase PDIA5 to modulate chemoresistance, *Mol. Cell. Biol.*, 2014, **34**, 1839–1849.
  - 32 J. C. Young, The role of the cytosolic HSP70 chaperone system in diseases caused by misfolding and aberrant trafficking of ion channels, *Dis. Models & Mech.*, 2014, **7**, 319–329.
  - 33 M. Pagani, M. Fabbri, C. Benedetti, A. Fassio, S. Pilati, N. J. Bulleid, A. Cabibbo and R. Sitia, Endoplasmic reticulum oxidoreductin 1-lbeta (ERO1-Lbeta), a human gene induced in the course of the unfolded protein response, *J. Biol. Chem.*, 2000, **275**, 23685–23692.
  - 34 T. van Laar, A. J. van der Eb and C. Terleth, Mif1: a missing link between the unfolded protein response pathway and ER-associated protein degradation?, *Curr. Protein Pept. Sci.*, 2001, **2**, 169–190.
  - 35 P. Walter and D. Ron, The unfolded protein response: from stress pathway to homeostatic regulation, *Science*, 2011, **334**, 1081–1086.
  - 36 D. Kummel, A. Oeckinghaus, C. Wang, D. Krappmann and U. Heinemann, Distinct isocomplexes of the TRAPP trafficking factor coexist inside human cells, *FEBS Lett.*, 2008, **582**, 3729–3733.
  - 37 Y. Yamamoto and T. Sakisaka, Molecular machinery for insertion of tail-anchored membrane proteins into the endoplasmic reticulum membrane in mammalian cells, *Mol. Cell*, 2012, **48**, 387–397.
  - 38 Y. Yamamoto, A. Yoshida, N. Miyazaki, K. Iwasaki and T. Sakisaka, Arl6IP1 has the ability to shape the mammalian ER membrane in a reticulon-like fashion, *Biochem. J.*, 2014, **458**, 69–79.
  - 39 Y. Peng and L. Puglielli, N-lysine acetylation in the lumen of the endoplasmic reticulum: A way to regulate autophagy and maintain protein homeostasis in the secretory pathway, *Autophagy*, 2016, **12**, 1051–1052.
  - 40 S. Kadowaki, S. Meguro, Y. Imaizumi, H. Sakai, D. Endoh and M. Hayashi, Role of p38 Mapk in development of acute hepatic injury in Long-Evans Cinnamon (LEC) rats, an animal model of human Wilson's disease, *J. Vet. Med. Sci.*, 2013, **75**, 1551–1556.
  - 41 C. W. Lai, J. H. Otero, L. M. Hendershot and E. Snapp, ERdj4 protein is a soluble endoplasmic reticulum (ER) DnaJ family protein that interacts with ER-associated degradation machinery, *J. Biol. Chem.*, 2012, **287**, 7969–7978.
  - 42 A. H. Lee, N. N. Iwakoshi and L. H. Glimcher, XBP-1 regulates a subset of endoplasmic reticulum resident chaperone genes in the unfolded protein response, *Mol. Cell. Biol.*, 2003, **23**, 7448–7459.
  - 43 A. Higa and E. Chevet, Redox signaling loops in the unfolded protein response, *Cell. Signalling*, 2012, **24**, 1548–1555.
  - 44 D. Morito and K. Nagata, ER Stress Proteins in Autoimmune and Inflammatory Diseases, *Front. Immunol.*, 2012, **3**, 48.
  - 45 R. S. Polishchuk, M. Castrorao and E. V. Polishchuk, Shaping tubular carriers for intracellular membrane transport, *FEBS Lett.*, 2009, **583**, 3847–3856.
  - 46 V. A. Assimon, A. T. Gillies, J. N. Rauch and J. E. Gestwicki, Hsp70 protein complexes as drug targets, *Curr. Pharm. Des.*, 2013, **19**, 404–417.